Electronic Supplementary Material (ESI) for Dalton Transactions.

Electronic Supplementary Information

Thioether Sulfur Bound [Cu_2] Complexes Showing Catechol Oxidase Activity and DNA Cleaving Behaviour

Manisha Das,[a] Zeenat Afsan,[b] Dipmalya Basak,[a] Farukh Arjmand[b] and Debashis Ray*[a]

[a]*Department of Chemistry, Indian Institute of Technology, Kharagpur 721 302, India*

[b]*Department of Chemistry, Aligarh Muslim University, Aligarh, 202002, UP, India*

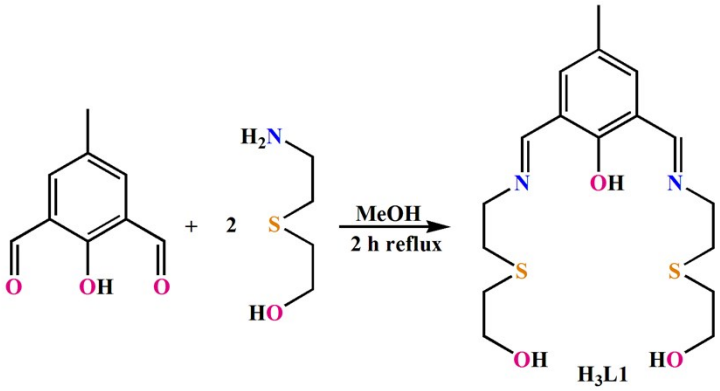

Scheme S1 Synthetic step for H_3L1.

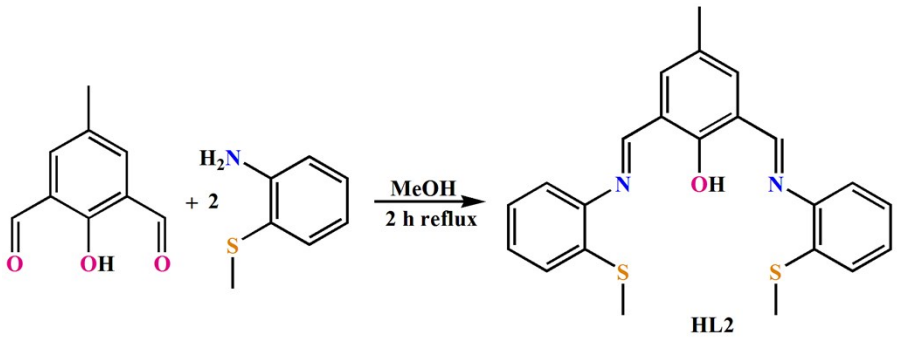

Scheme S2 Synthetic step for HL2.

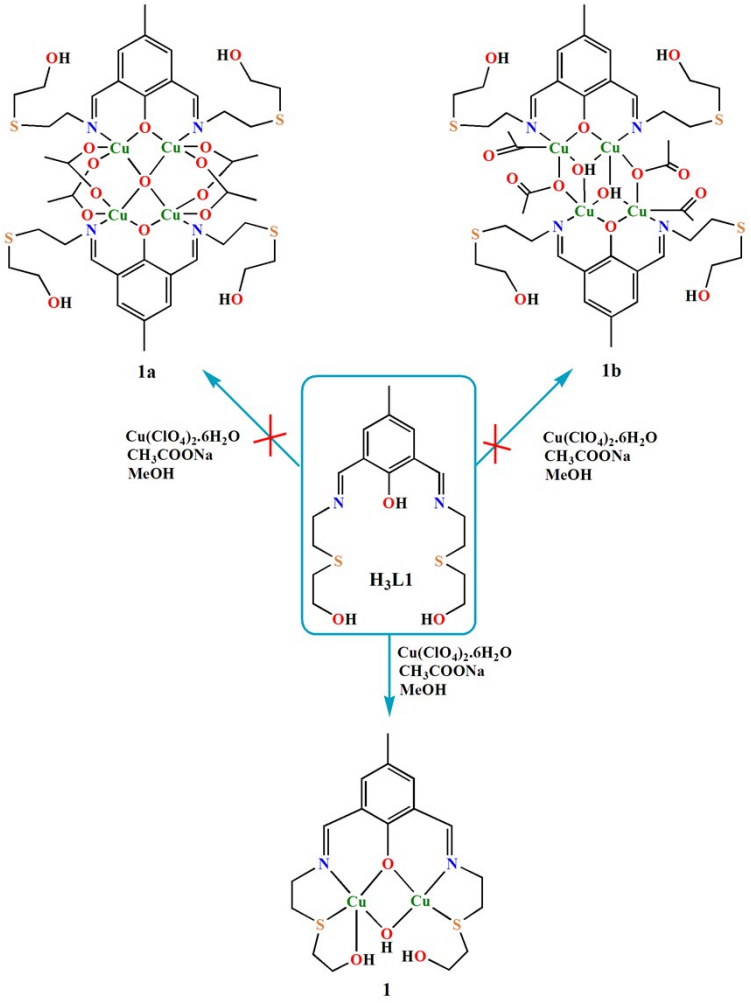

Scheme S3 Aggregation inhibited reaction path for **1**.

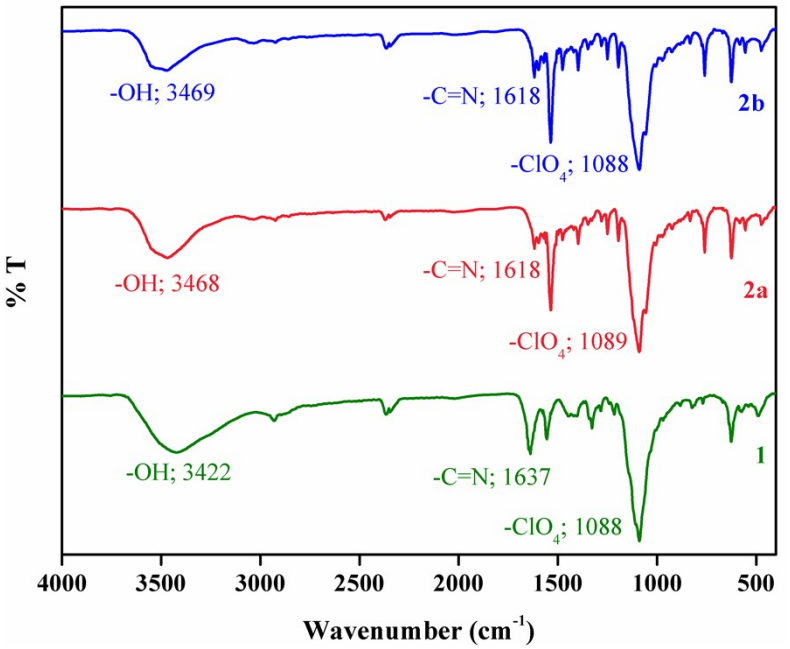

Fig. S1 FTIR Spectra of **1**-**2b**.

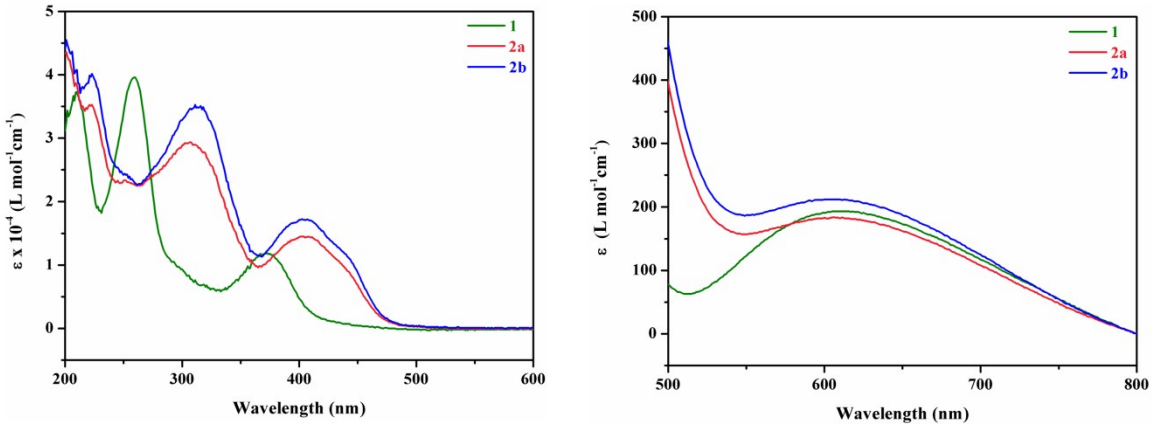

Fig. S2 Charge transfer (left) and d-d transition (right) bands for **1**-**2b**.

Hirshfeld Surfaces Analyses. In order to get an additional insight into a role of the crystal packing forces in stabilization of the structures of **1**, **2a** and **2b**, we have conducted a comparative Hirshfeld surface analysis of the molecules.[R1] The surfaces are useful for gaining information about different intermolecular interactions, and to identify and quantify these interactions. The Hirshfeld surface emerged from an attempt to define the space occupied by a molecule in a crystal for the purpose of partitioning the crystal electron density into molecular fragments. The analysis using crystal structure data provides a visual picture, where the various

types of interactions can be clearly identified by the shapes, contours and colours provided by the computation and has been generated from CrystalExplorer 3.1.[R2] It provided insight into the crystal packing forces within the molecular crystal. The Hirshfeld surfaces of **1**–**2b** mapped over d_{norm} (–0.5 to 1.5 Å) are presented in Fig. S3. The surfaces of **1**–**2b** mapped over the curvedness (–4.0 to 0.4 Å) and shape index (–1.0 to 1.0 Å) are displayed in Fig. S4. The deep red visible spots on the d_{norm} surfaces are due to the hydrogen bonding contacts and other visible spots are indicative of H···H contacts. The dominant O···H interactions are viewed as a bright red area and C–H···O interactions are as light red spots (Fig. S3). The inside of the bimetallic region in all cases is mainly of white colour and that the surface of the bridging anion has also many white regions which have contacts around the van der Waals distance. The curvedness surface indicates electron density surface curves around the molecular interactions. Shape index and curvedness surface are used to identify planner stacking (π···π) interactions. In the shape index surface red and blue triangle indicate π···π interaction is almost identically present in the crystal structures. The convex region formed due to the carbon atoms present in the benzene ring of the molecule inside the surface are represented by blue triangles while the red triangle represents concave regions due to the carbon atoms of the π stacked molecule above it. The planner green region separated by blue lines present in the curvedness surface is another characteristic of π···π interaction.

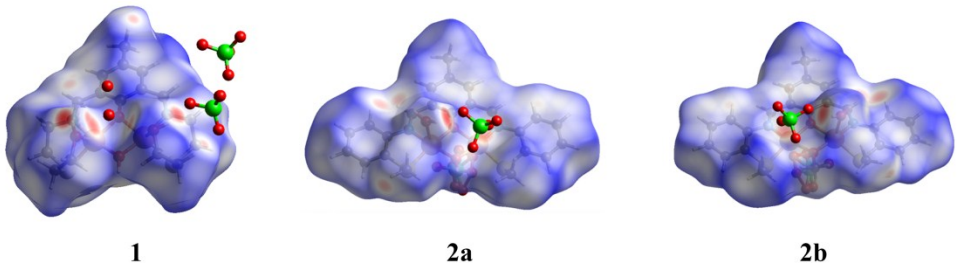

Fig. S3 Hirshfeld surfaces mapped over d_{norm} for **1**–**2b**.

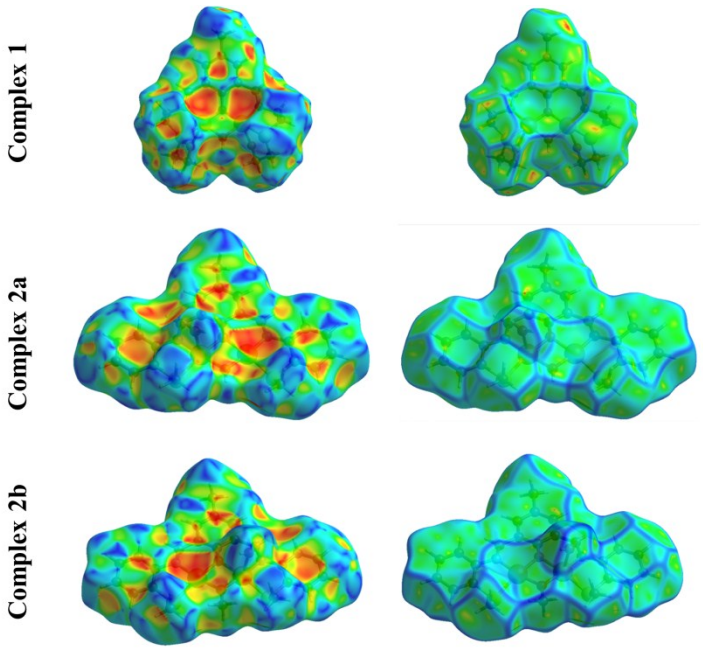

Fig. S4 Hirshfeld surfaces mapped over shape index (left) and curvedness (right) for **1**–**2b**.

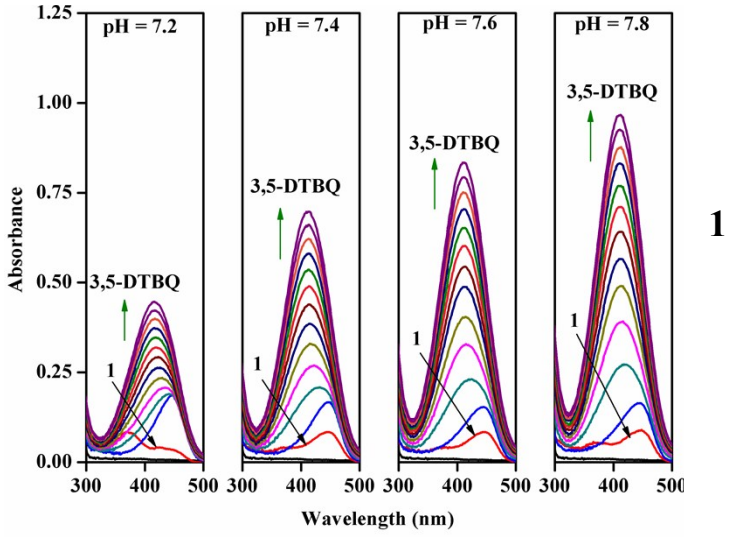

1

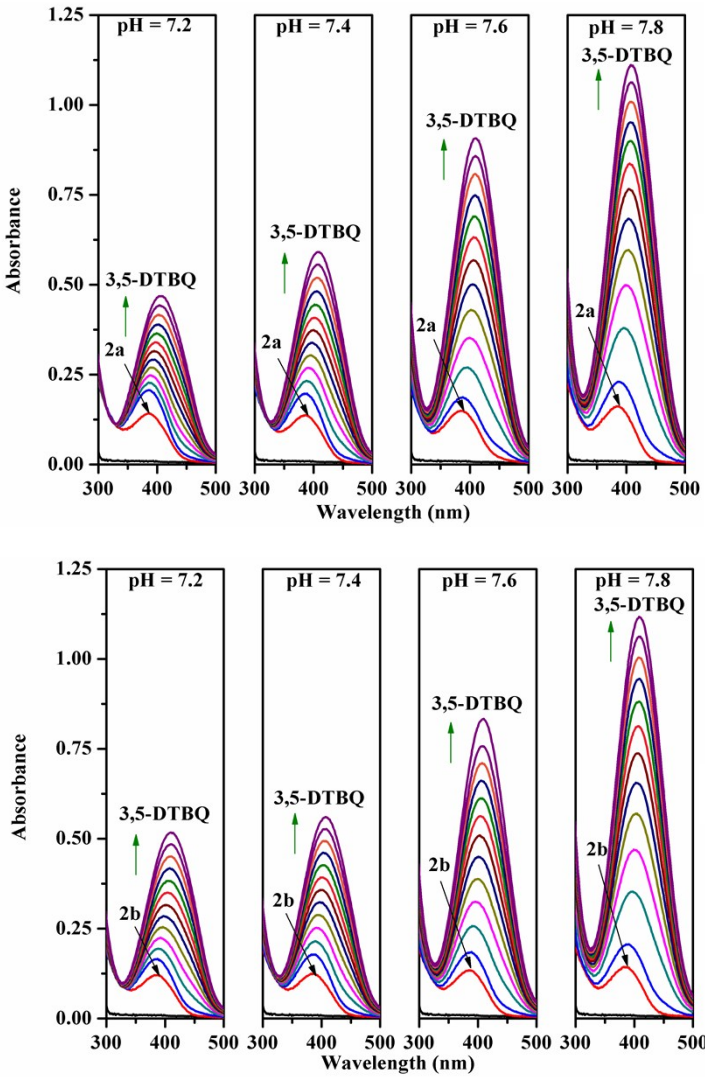

Fig. S5. Time dependent spectral changes for **1** (top), **2a** (middle) and **2b** (bottom) upon addition of 100 equivalents of 3,5-DTBCH_2 in MeCN-H_2O (1:1) at *pH* 7.2–7.8.

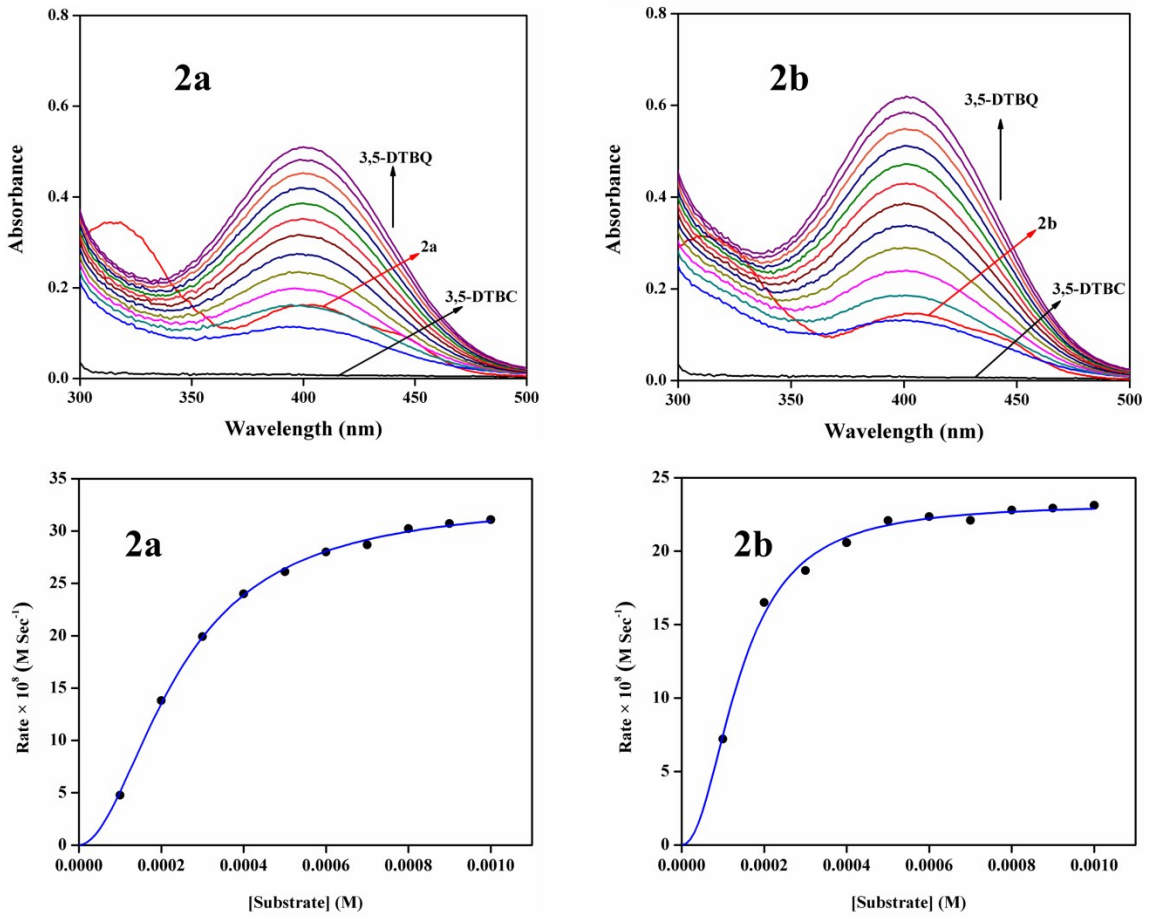

Fig. S6 Top: Time dependent spectral changes for **2a** (left) and **2b** (right) upon addition of 100 equivalents of 3,5-$DTBCH_2$ in MeOH. Bottom: Kinetic plots for **2a** (left) and **2b** (right) in MeOH.

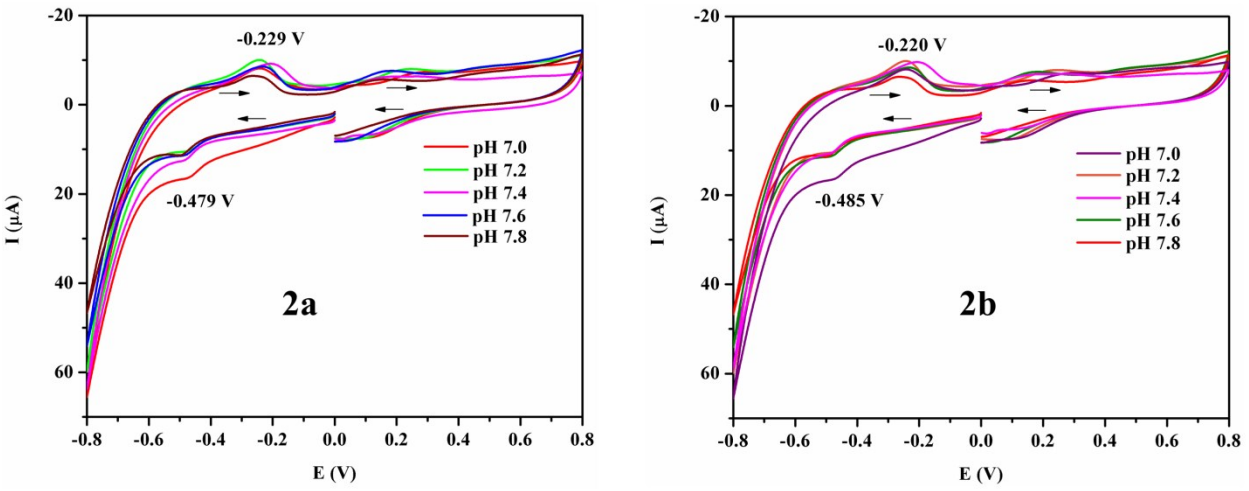

Fig. S7 Cyclic voltammograms for **2a** (left) and **2b** (right) at *pH* 7.0, 7.2, 7.4, 7.6 and 7.8 (maintained by appropriate 50 mM Tris-HCl buffer solutions) in MeCN-H_2O (1:1) under N_2 atmosphere at Pt disc working electrode, Ag/AgCl reference electrode and Pt wire counter electrode.

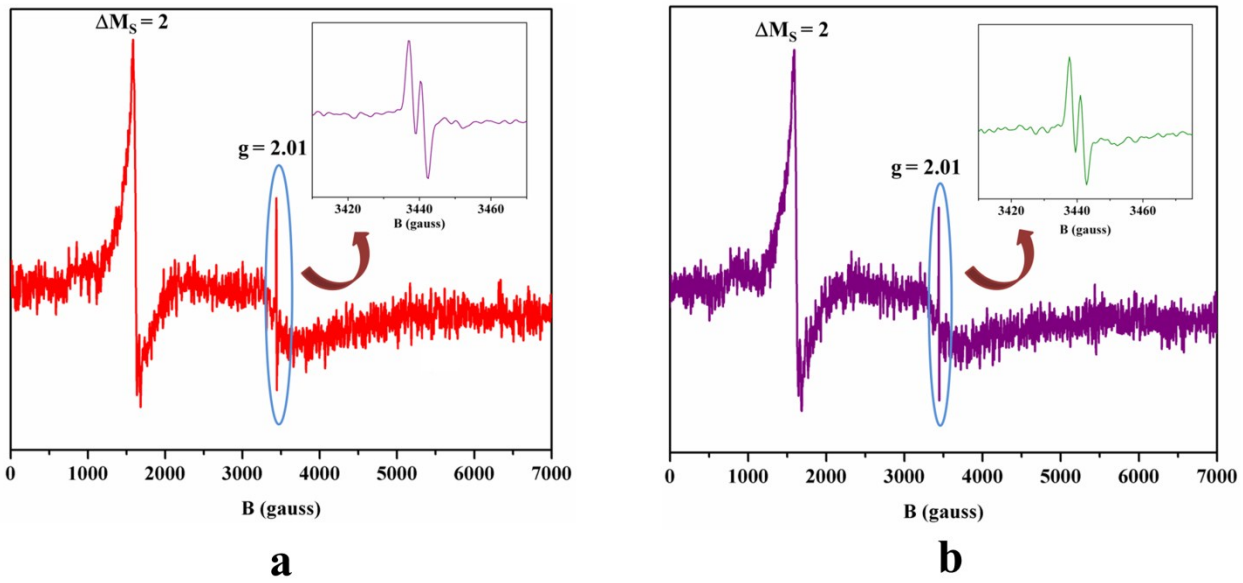

Fig. S8 EPR spectra at 298 K of (a) **2a** + 100 equivalent 3,5-DTBCH$_2$ and (b) **2b** + 100 equivalent 3,5-DTBCH$_2$ in MeOH.

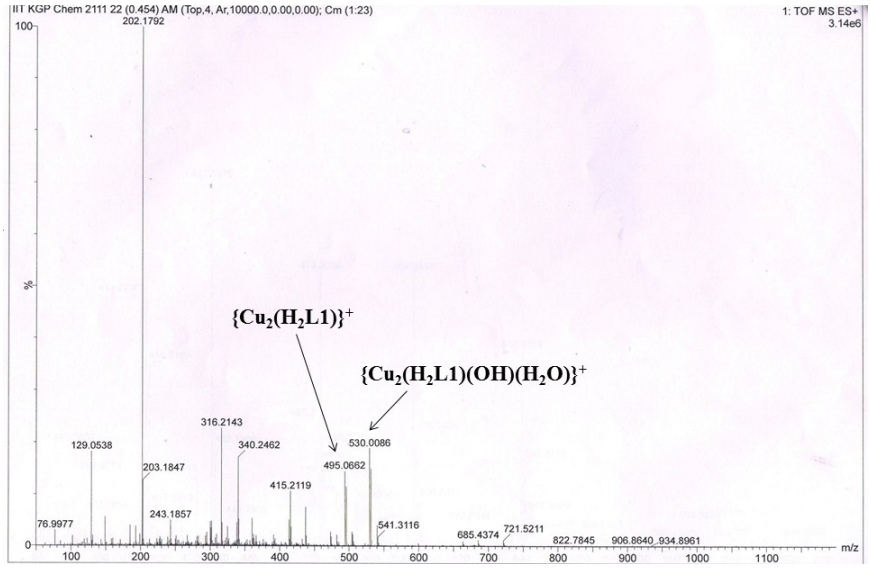

Fig. S9. ESI-MS spectrum of **1** in MeOH.

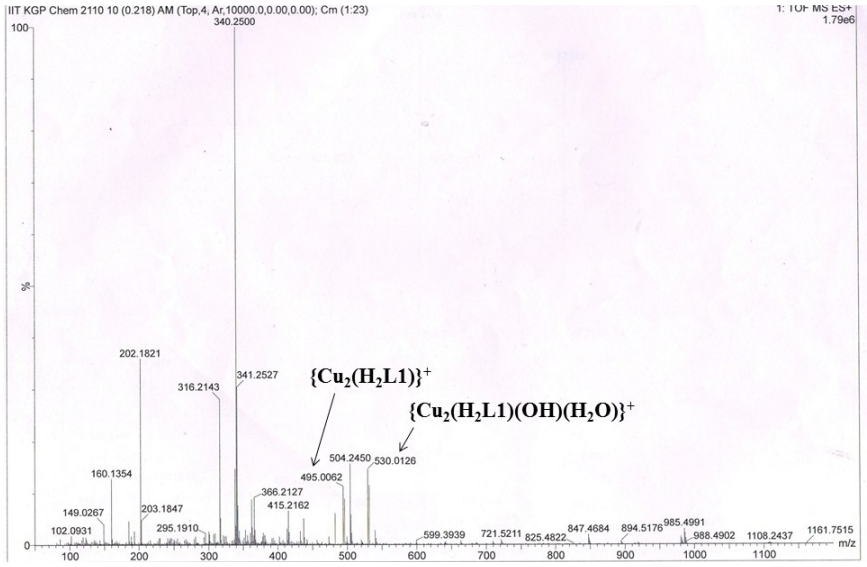

Fig. S10 ESI-MS spectrum of **1** in MeCN-H_2O (1:1).

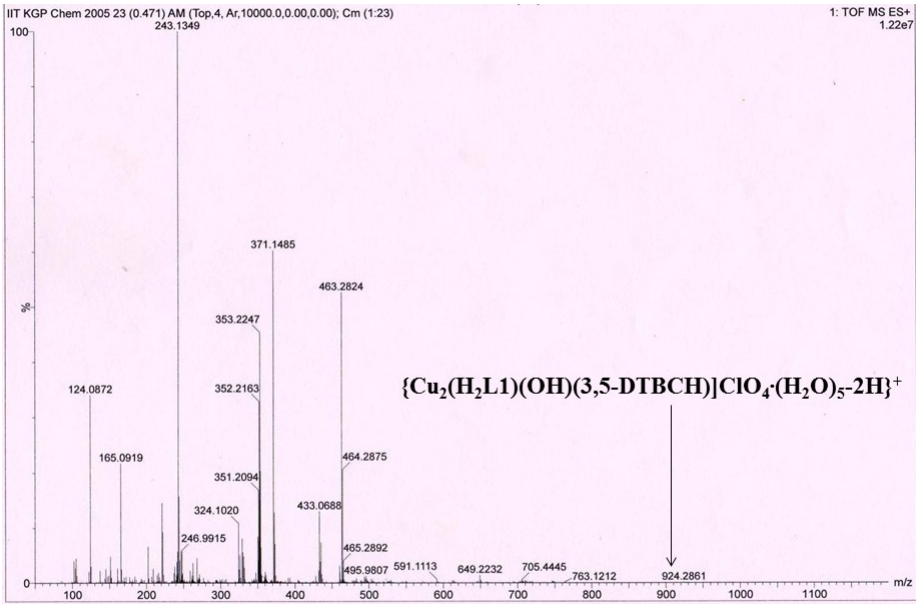

Fig. S11 ESI-MS spectrum of a (1:100) mixture **1** and 3,5-$DTBCH_2$ in MeCN-H_2O (1:1) at *pH* 7.0 after 5 min of mixing.

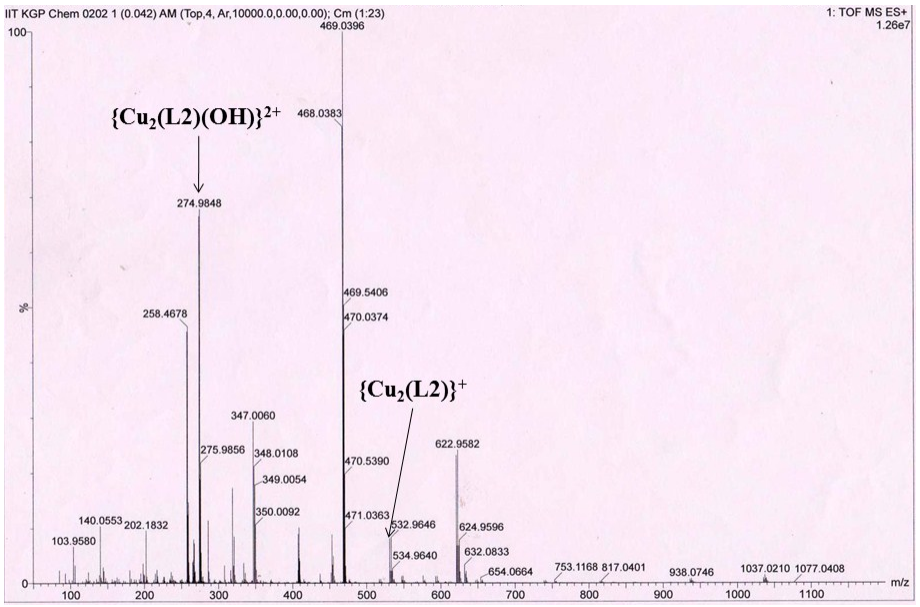

Fig. S12 ESI-MS spectrum of **2a** in MeCN-H_2O (1:1).

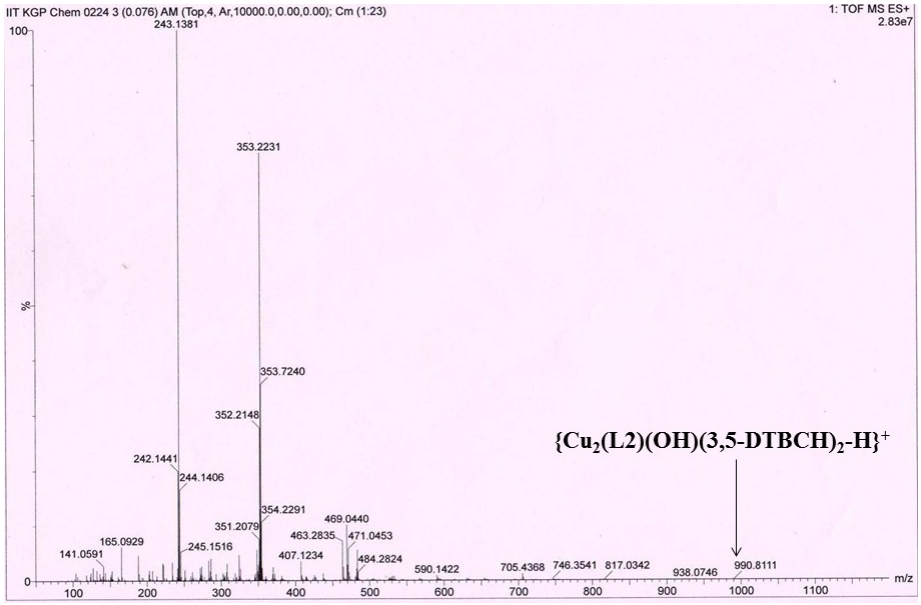

Fig. S13 ESI-MS spectrum of (1:100) mixture of **2a** and 3,5-$DTBCH_2$ in MeCN-H_2O (1:1) at *pH* 7.0 after 5 min of mixing.

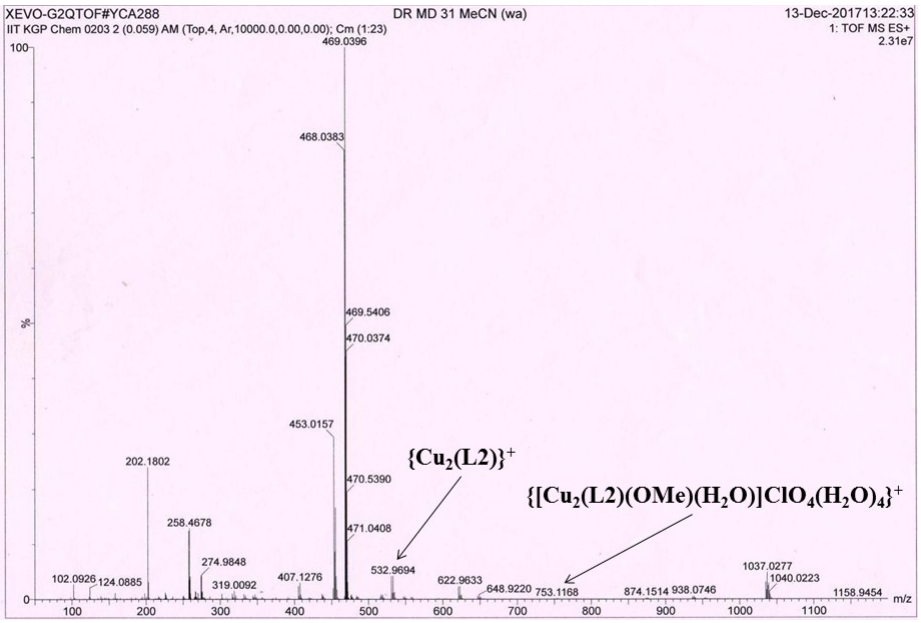

Fig. S14 ESI-MS spectrum of **2b** in MeCN-H_2O (1:1).

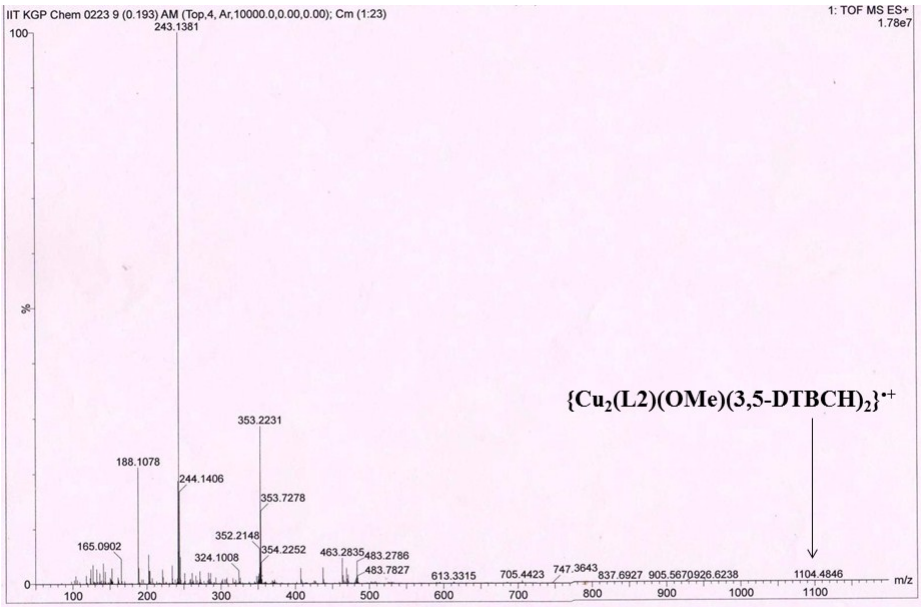

Fig. S15 ESI-MS spectrum of (1:100) mixture of **2b** and 3,5-$DTBCH_2$ in MeCN-H_2O (1:1) at *pH* 7.0 after 5 min of mixing.

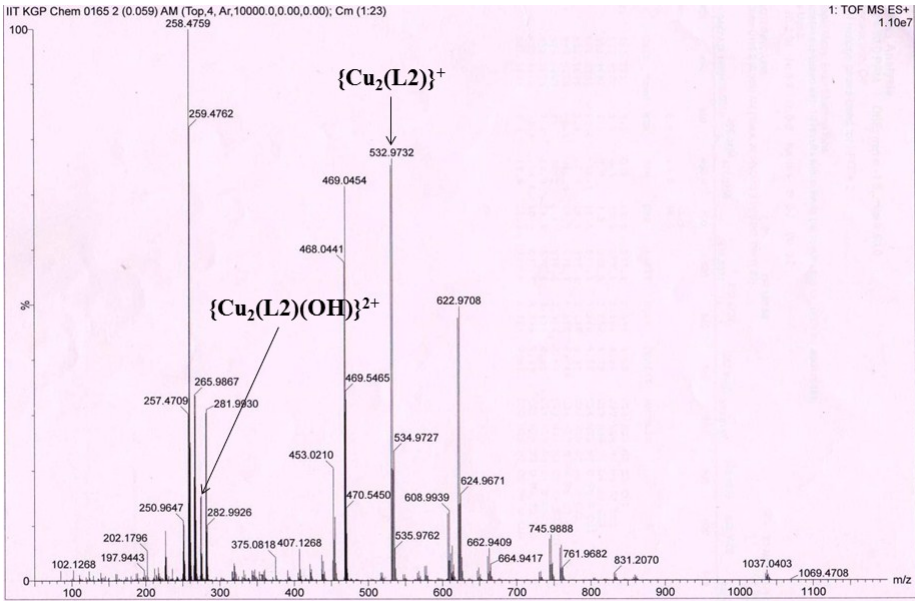

Fig. S16 ESI-MS spectrum of **2a** in MeOH.

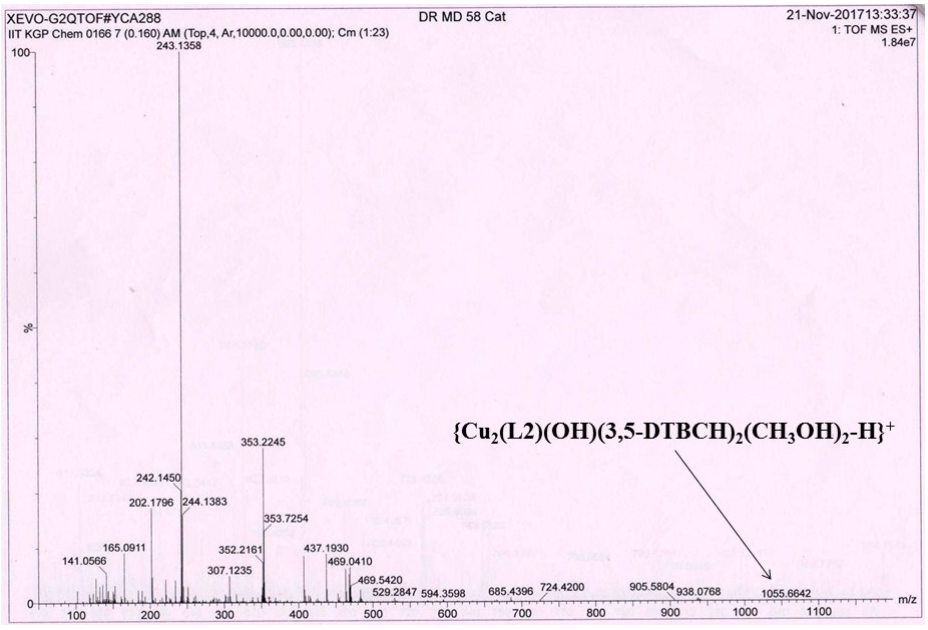

Fig. S17 ESI-MS spectra of (1:100) mixture of **2a** and 3,5-DTBCH$_2$ in MeOH after 5 min of mixing.

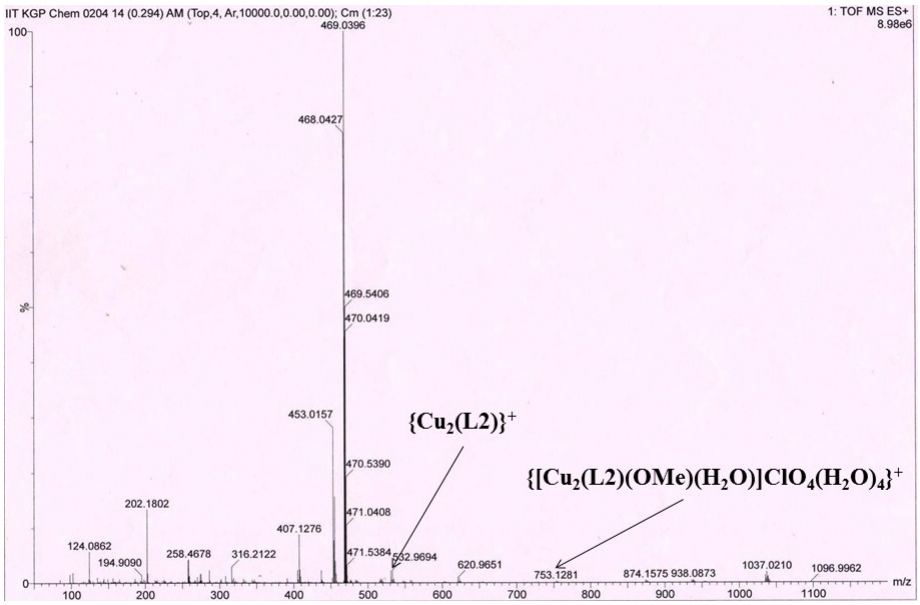

Fig. S18 ESI-MS spectra of **2b** in MeOH.

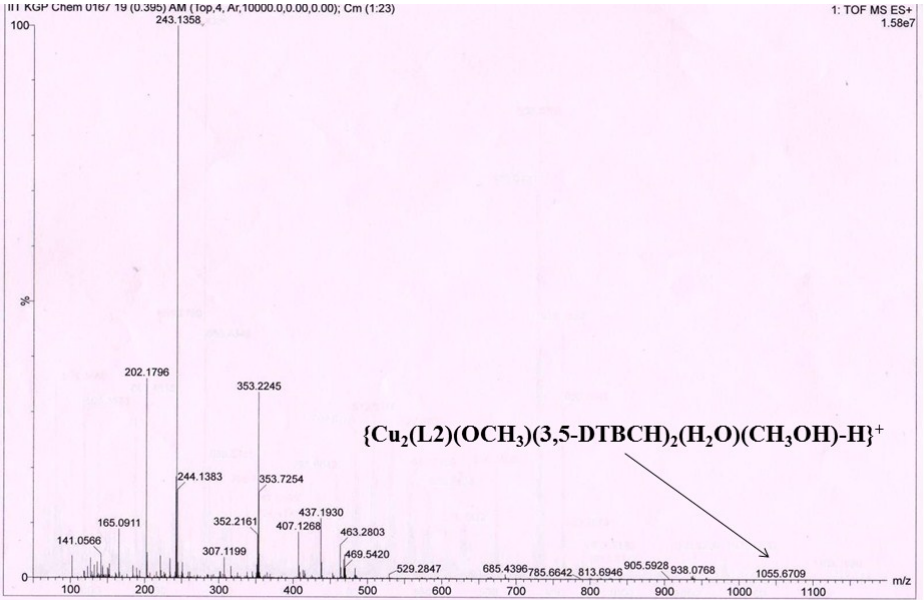

Fig. S19 ESI-MS spectra of (1:100) mixture of **2b** and 3,5-DTBCH$_2$ in MeOH after 5 min of mixing.

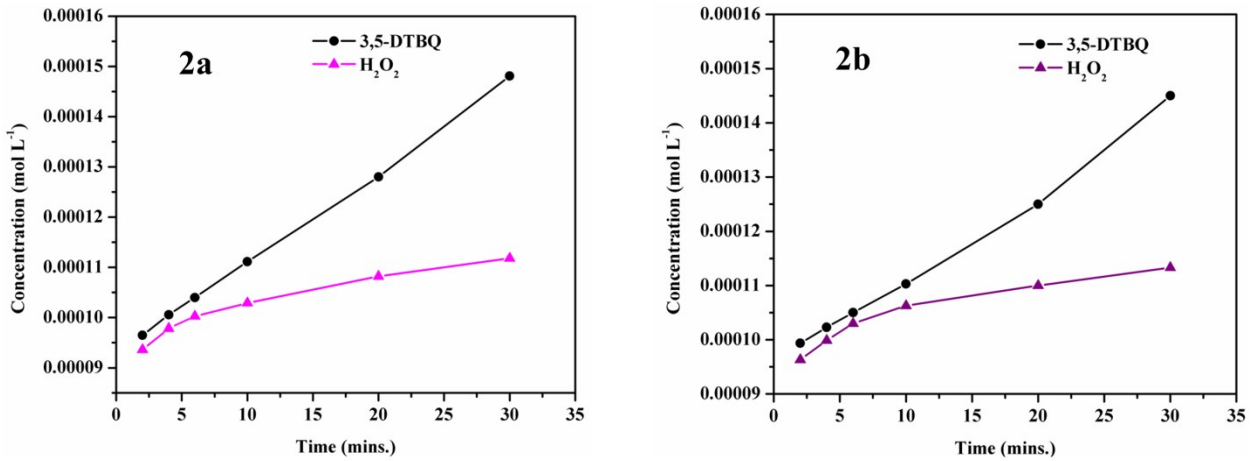

Fig. S20 Estimation of H_2O_2 after 2, 4, 6, 10, 20 and 30 minutes of mixing with 3,5-DTBCH_2 in MeOH for **2a** and **2b**.

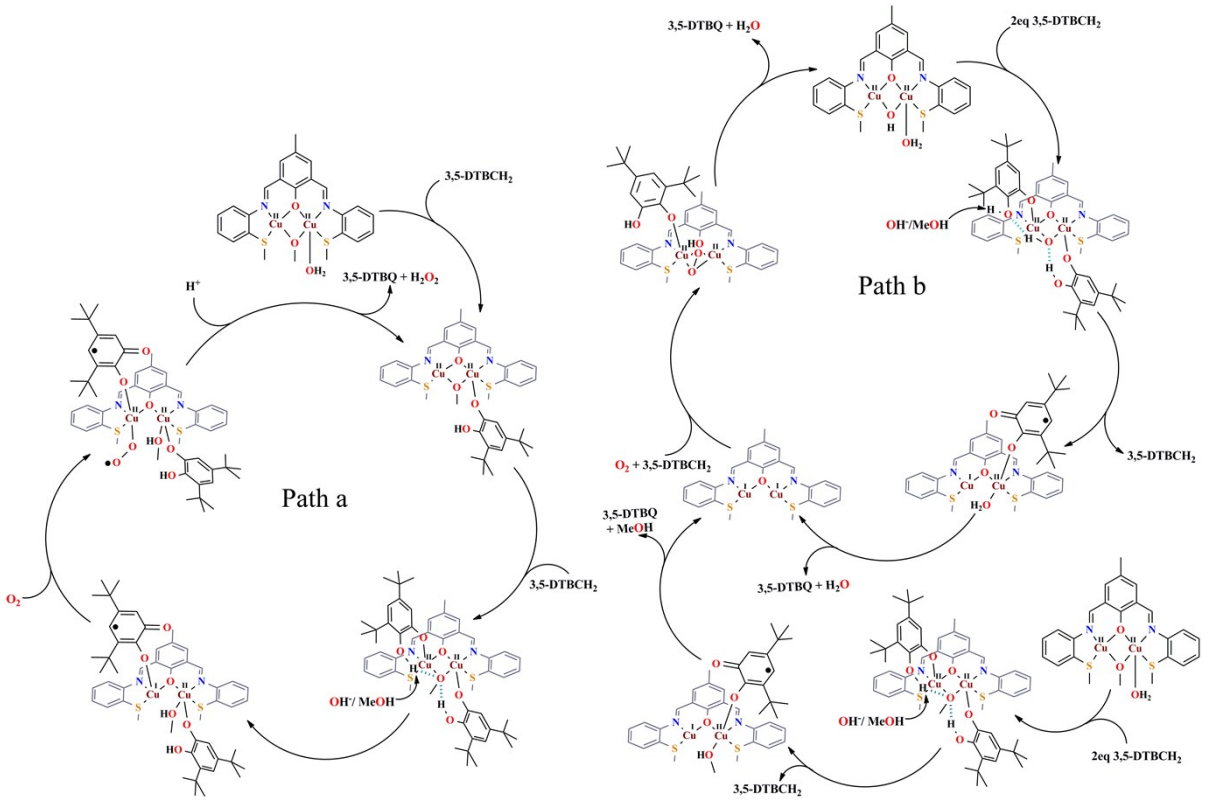

Scheme S4 Two different catalytic pathways ‘a’ and ‘b’ for **2b**.

Table S1 Selected bond distances (Å) and angles (º) in **1**, **2a** and **2b**

Bond lengths (Å)					
Complex **1**					
Cu1 − O1	1.972(4)	Cu2 – O1	1.973(4)	Cu2 – S2	2.3473(16)
Cu1 – O2	1.880(4)	Cu2 – O2	1.875(4)	Cu1 – Cu2	2.9466(9)
Cu1 – N1	1.926(5)	Cu2 – O4	2.350(5)		
Cu1 – S1	2.3212(16)	Cu2 – N2	1.923(5)		
Complex **2a**					
Cu1 − O1	1.9424(18)	Cu2 –O1	1.9400(19)	Cu2 – S2	2.2677(11)
Cu1 – O2	1.9136(19)	Cu2 – O2	1.9264(19)	Cu1 – Cu2	2.9534(12)
Cu1 – N1	1.948(2)	Cu2 – O11	2.393(2)		
Cu1 – S1	2.2738(9)	Cu2 – N2	1.950(2)		
Complex **2b**					
Cu1 − O1	1.957(4)	Cu2 – O1	1.957(4)	Cu2 – O3	2.366(6)
Cu1 – O2	1.895(5)	Cu2 – O2	1.900(4)	Cu1 – Cu2	2.982(2)
Cu1 – N1	1.945(5)	Cu2 – N2	1.944(5)		
Cu1 – S1	2.293(2)	Cu2 – S2	2.280(3)		
Bond angles (°)					
Complex **1**					
O1–Cu1–N1	92.09(17)	O1−Cu1−S1	171.56(13)	O1−Cu2−O4	109.46(16)
O1−Cu2−S2	169.34(13)	O2−Cu1−O1	79.26(16)	O2−Cu2−N1	171.34(18)
O2–Cu1–S1	98.65(13)	O2−Cu2−O1	79.36(16)	O2−Cu2−N2	170.43(18)
O2–Cu2–O4	92.29(19)	O2−Cu2−S2	100.05(13)	N1−Cu1−S1	89.97(14)
N2−Cu2−O1	91.31(17)	N2−Cu2−S2	88.71(14)	N2−Cu2−O4	92.86(19)
Cu1−O1−Cu2	96.67(16)	Cu2−O2−Cu1	103.38(19)		
Complex **2a**					
O1–Cu1–N1	93.02(8)	O2−Cu1−N1	172.88(8)	N1−Cu1−S1	87.85(7)

O1−Cu1−S1	166.81(6)	O2−Cu1−S1	99.25(6)	N2−Cu2−S2	88.14(7)
O1–Cu2–N2	94.16(8)	O2−Cu2−O1	79.70(8)	N2−Cu2−O11	87.34(9)
O1–Cu2–S2	168.18(6)	O2−Cu2−N2	172.32(8)	S2−Cu2−O11	98.58(7)
O1−Cu2−O11	93.11(9)	O2−Cu2−S2	96.95(6)	Cu1−O1−Cu2	99.05(8)
O2−Cu1−O1	79.96(8)	O2−Cu2−O11	97.53(9)	Cu1−O2−Cu2	100.55(9)
Complex **2b**					
O1−Cu1−S1	165.37(15)	O2−Cu2−O1	78.15(18)	N2–Cu2–O1	93.5(2)
O1−Cu2−S2	168.02(15)	O2−Cu2−O3	95.3(2)	N2−Cu2−O3	89.3(2)
O1−Cu2−O3	93.4(2)	O2−Cu2−N2	170.6(2)	N2−Cu2−S2	88.26(18)
O2−Cu1−O1	78.25(18)	O2−Cu2−S2	99.11(16)	S2−Cu2−O3	98.49(16)
O2−Cu1−N1	170.87(18)	N1−Cu1−O1	92.66(18)	Cu1−O1−Cu2	99.3(2)
O2−Cu1−S1	101.92(16)	N1−Cu1−S1	87.09(16)	Cu1−O2−Cu2	103.6(2)

Table S2 Hydrogen bonding parameters for **1**, **2a** and **2b**

Interactions	Type of H-bond	D–H (Å)	D···A (Å)	H···A (Å)	D–H···A (Å)
Complex **1**					
O2–H2···O8		0.89	2.850(2)	2.02	156
O3–H3A···O6		0.82	2.859(19)	2.08	158
O1W–H1WA···O4		0.85	2.716(10)	2.27	113
O1W–H1WB···O3		0.85	2.791(11)	2.40	108
O2W–H2WA···O1W		0.85	2.820(14)	1.97	176
O2W–H2WB···O9		0.85	2.940(15)	2.09	176
Complex **2a**					
O11–H11A···O6		0.93	2.871(4)	2.05	146
O11–H11B···O9		0.93	2.674(10)	1.78	161
O2–H2···O3		0.86	3.104(3)	2.36	146
Complex **2b**					
O3–H3A···O4		0.93	2.800(9)	1.97	148
O3–H3B···O9		0.93	2.68(3)	1.79	158

References

R1. M.A. Spackman and D. Jayatilaka, *Cryst. Eng. Comm.*, 2009, **11**, 19−32.

R2. S. K. Wolff, D. J. Grimwood, J. J. McKinnon, M. J. Turner, D. Jayatilaka and M. A. Spackman, Crystal Explorer 3.1, University of Western Australia, 2012